



Universal Conductance Scaling of Andreev Reflections Using a Dissipative Probe

Donghao Liu,¹ Gu Zhang,² Zhan Cao,² Hao Zhang^{1,2,3} , and Dong E. Liu^{1,2,3,*} 

¹State Key Laboratory of Low Dimensional Quantum Physics, Department of Physics, Tsinghua University, Beijing 100084, China

²Beijing Academy of Quantum Information Sciences, Beijing 100193, China

³Frontier Science Center for Quantum Information, Beijing 100184, China



(Received 2 November 2021; accepted 25 January 2022; published 18 February 2022)

The Majorana search is caught up in an extensive debate about the false-positive signals from nontopological Andreev bound states. We introduce a remedy using the dissipative probe to generate electron-boson interaction. We theoretically show that the interaction-induced renormalization leads to significantly distinct universal zero-bias conductance behaviors, i.e., distinct characteristic power law in temperature, for different types of Andreev reflections, that show a sharp contrast to that of a Majorana zero mode. Various specific cases have been studied, including the cases in which two charges involved in an Andreev reflection process maintain or lose coherence, and the cases for multiple Andreev bound states with or without a Majorana. A transparent list of conductance features in each case is provided to help distinguish the observed subgap states in experiments, which also promotes the identification of Majorana zero modes.

DOI: [10.1103/PhysRevLett.128.076802](https://doi.org/10.1103/PhysRevLett.128.076802)

Introduction.—Quantum tunneling [1] has been used as a very powerful method to study quantum materials and quantum devices. However, if obtained using noninteracting probe and target, the tunneling signal is usually very sensitive to contaminants that potentially induce nonuniversal behaviors. As an important example, the tunneling spectroscopy signals used in detecting Majorana zero modes (MZMs) [2,3] in semiconductor-superconductor heterostructures [4–6] should give a quantized zero-bias conductance peak [7–10] and a robust quantized plateau by varying all relevant control parameters. However, the current experimental results [11–28] are far from the ideal predictions. One of the key reasons is that such a noninteracting Majorana detection platform is easily contaminated by junction and disorder-induced Andreev bound states (ABSs) [29–37] that cause nonrobust signals.

As a possible remedy, interaction, known as a method to sharpen transition between different fixed points, can be introduced to classify different physics under the interaction renormalization [38]. Indeed, different physics emerges near fixed points that belong to distinct interaction-dependent universality classes. One of the simplest schemes to introduce interaction is to consider a dissipative electromagnetic environment, e.g., applying an ohmic resistance in series with the tunneling junction, and causing effective electron-boson interaction [39]. With ohmic dissipation, the tunneling conductance exhibits dissipation-dependent power-law scaling behaviors [39]. Various kinds of dissipation-influenced charge transport in mesoscopic systems have been studied both experimentally [40–43] and theoretically [44–56].

Main results.—Here, we focus on the hybrid semiconductor-superconductor nanowire device for the

detection of Majorana resonance. The dissipative tunneling into a MZM was proposed as a Majorana signature filter [48] by one of the authors. It is believed that junction and/or disorder-induced fermionic ABSs dominate the phase diagram of the current nanowire devices [36,57]. Therefore, it is an interesting topic to study the dissipative interacting probe for different types of ABSs and obtain their universal scaling behaviors under renormalization to distinguish between ABSs and the real MZM. Following this motivation, we map the dissipative tunneling into ABSs to a Coulomb gas model, and find that the zero-bias conductance has special power-law dependence on temperature T . In addition, we find that the coherence between electron and hole after the Andreev reflection will significantly affect the power-law behaviors; therefore, the measurement of the power law could be applied to detect the coherence after the Andreev reflection. We show that the dissipation can cause significantly different universal behaviors according to their characteristic power law as summarized in Table I for different types of Andreev reflections and MZM, where $r = Re^2/h$ is the dimensionless dissipation amplitude. Our result also potentially applies to other platforms using scanning tunneling microscope [58–62], where dissipation-induced dynamical Coulomb blockade features have been observed [63].

Model.—An illustration of the system is shown in Fig. 1. The dissipative tunneling to an ABS is achieved by tunnel coupling a lead to a nanowire. We consider the hybrid semiconductor-superconductor nanowire devices with finite magnetic field [4,5]. This type of device is recently well-studied for the detection of MZMs. Later we also call this hybrid device the “SC nanowire.” In reality, devices of

TABLE I. Universal scaling behaviors of different circumstances.

	Majorana [48]	ABS (coherent)	ABS (incoherent)	Normal state [39]
Qualitative	Enhancement	Decay	Decay	Decay
Universal scaling	$(2e^2/h) - G \sim T^{(2-4r/1+2r)}$	$G \sim T^{8r}$	$G \sim T^{4r}$	$G \sim T^{2r}$

this type are easily contaminated by disorders in the junction or the nanowire bulk, and the disorder-induced trivial ABSs potentially produce false-positive signals in the standard tunneling experiments. The system is also coupled to a dissipative bath, which can be achieved by replacing part of the electrode with a long and thin resistive metal strip (with resistance R ; red in Fig. 1). The tunnel gate controls the coupling between the lead and the SC nanowire. An equivalent circuit diagram is shown in Fig. 1.

The whole system includes four parts: the SC nanowire, the lead, the tunneling part, and the dissipative environment. For the SC nanowire, we focus on the case with an ABS localized at the left side of the nanowire, and its Hamiltonian can be written as $H_{\text{wire}} = \epsilon a^\dagger a + \text{const}$, where a is the fermionic quasiparticle operator for the ABS. Its energy is inside the superconducting gap $\epsilon < \Delta$ and can reach $\epsilon \rightarrow 0$ by adjusting experimental variables, e.g., gate voltages or magnetic field. The lead can be described by the Hamiltonian of spinful fermions with dispersion linearized close to the Fermi energy:

$$H_{\text{lead}} = v_F \sum_{\sigma=\uparrow/\downarrow} \int_{-\infty}^0 dx \psi_{L,\sigma}^\dagger i \partial_x \psi_{L,\sigma} - \psi_{R,\sigma}^\dagger i \partial_x \psi_{R,\sigma}, \quad (1)$$

where $\psi_{L,\sigma}(x)$ and $\psi_{R,\sigma}(x)$ are fermion operators for the left-moving and right-moving modes with spin σ at point x in the lead. Counting the degrees of freedom of the particle (hole) and the spin, there are a total of four conducting channels in the lead. The tunneling part of the Hamiltonian can be expressed as

$$H_T = [\psi_\uparrow^\dagger(0)\psi_\downarrow^\dagger(0)] \begin{pmatrix} t_{e\uparrow} & t_{h\uparrow}^* \\ t_{e\downarrow}^* & t_{h\downarrow} \end{pmatrix} \begin{pmatrix} a \\ a^\dagger \end{pmatrix} e^{-i\varphi} + \text{H.c.}, \quad (2)$$

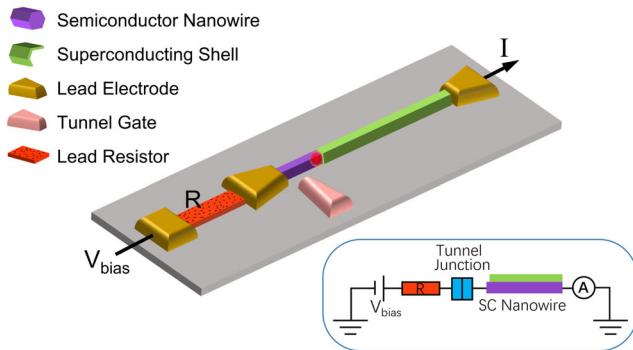


FIG. 1. Illustration of the system setup. The inset is the equivalent circuit. A bias voltage V_{bias} is applied on the lead.

where $\psi_\sigma(0) = \psi_{L,\sigma}(0) + \psi_{R,\sigma}(0)$. Breaking the spin rotation and time reversal symmetries, we need four independent tunneling parameters— $t_{e\uparrow}$, $t_{e\downarrow}$, $t_{h\uparrow}$, $t_{h\downarrow}$ —to describe an arbitrary ABS, as shown in Fig. 2(a). The operator $e^{-i\varphi}$ is conjugate to the charge fluctuation Q of the junction capacitance, following $[\varphi, Q] = ie$, and thus accompanies nanowire-superconductor charge transport. It couples bilinearly to the dissipative environment represented by a set of harmonic oscillators (i.e., $[q_n, \varphi_n]$ with oscillator frequency $\omega_n = 1/\sqrt{L_n C_n}$) [39,64,65]: $H_{\text{env}} = Q^2/2C + \sum_{n=1}^N [q_n^2/2C_n + (\hbar/e^2)^2(\varphi - \varphi_n)^2/2L_n]$, where C_n and L_n , respectively, refer to the effective capacitance and impedance of the n th dissipative mode. Here the dissipation is manifested through interaction with bosonic modes. The influence of dissipation in the diffusive regime has been studied in Ref. [66] by considering a normal diffusive metal-superconductor setup.

Effective action and Coulomb gas model.—Overall, the partition function of this tunnel junction coupled to the dissipative environment is

$$Z = \int [D\Phi_\uparrow][D\Phi_\downarrow][D\varphi][Da] e^{-S_{\text{eff}}} e^{-S_T}, \quad (3)$$

where S_T is the action of the tunneling part $S_T = \int_0^\beta dt L_T$ with the tunneling Lagrangian L_T directly obtained from Eq. (2), and β is the temperature inverse. After a spatial integral, the effective action becomes $S^{\text{eff}} = (1/\beta) \times \sum_{\omega_n} |\omega_n| [\sum_{\sigma} |\Phi_\sigma(\omega_n)|^2 + |\varphi(\omega_n)|^2/2r]$, with the first and the second terms in the brackets from the lead and the environment parts respectively. For later convenience, we define $r = Re^2/h$ as the dimensionless dissipation.

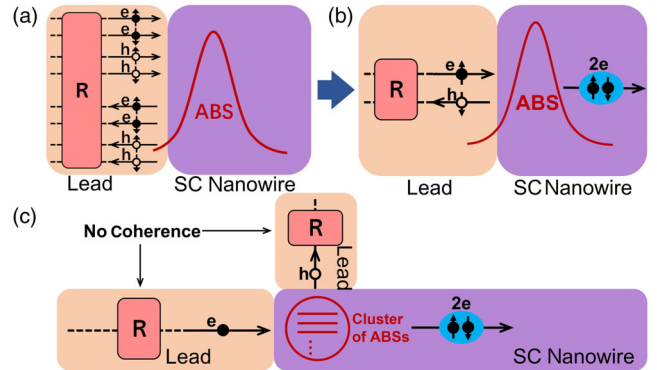


FIG. 2. (a) All possible processes. (b) Leading process after RG. (c) Incoherent dissipative Andreev reflection via a cluster of ABSs.

$\Phi_\sigma(x)$ is the chiral bosonic field from the standard bosonization [67]: $\psi_{L/R,\sigma}(x) = (1/\sqrt{2\pi\alpha})F_\sigma e^{-i\Phi_\sigma(\mp x)}$, where α is the short-distance cutoff and F_σ is the Klein factor. In the action S^{eff} , the lead part is obtained by integrating out fluctuations in $\Phi_\sigma(x)$ away from $x = 0$ [68–72], and the environment is obtained by integrating out the environmental degree of freedom [73].

By expanding the partition function Eq. (3) in the powers of tunneling part and then integrating out the bosonic field, we can obtain the Coulomb gas representation [68,69] for our model

$$Z = \sum_{\nu=\pm 1} \sum_n \sum_{\{q_i\}} \sum_{\{s_i\}} C_t \int_0^\beta d\tau_{2n} \int_0^{\tau_{2n}} d\tau_{2n-1} \times \dots \int_0^{\tau_3} d\tau_2 \int_0^{\tau_2} d\tau_1 e^{\sum_{i>j} V_{ij} e^{\nu\epsilon[\frac{\xi}{2} + \sum_i (-1)^i \tau_i]}}, \quad (4)$$

which describes a one-dimensional plasma of logarithmically interacting charges. The interaction V_{ij} has the form

$$V_{ij} = \frac{1}{2g} [q_i q_j + K_1 (q_i r_j + r_i q_j) + g s_i s_j + K_2 g (s_i r_j + r_i s_j)] \ln \left(\frac{\tau_i - \tau_j}{\tau_c} \right), \quad (5)$$

where the effective interaction parameter $g = (1 + 4Re^2/h)^{-1} = (1 + 4r)^{-1}$ and $1/\tau_c$ refers to the high-energy cutoff that changes during each renormalization group (RG) step. Three types of charges, i.e., q_i , s_i , and r_i are involved. The first two refer to the changes in charge and spin in the lead. The last one is from the ABS state. Initially, $K_1 = K_2 = 0$. They begin to grow in the presence of asymmetry, driving the system toward different fixed points [72].

RG analysis and scaling behaviors.—In the framework of the Coulomb gas model, the RG equation at weak tunneling coupling fixed point can be obtained from integrating out the degrees of freedom between τ_c and $\tau_c + d\tau_c$ (a real-space RG) [72]. The resulting RG equations yield

$$\frac{dK_1}{d \ln \tau_c} = -2\tau_c^2 [(|t_{e\uparrow}|^2 - |t_{h\uparrow}|^2 + |t_{e\downarrow}|^2 - |t_{h\downarrow}|^2) + (|t_{e\uparrow}|^2 + |t_{h\uparrow}|^2 + |t_{e\downarrow}|^2 + |t_{h\downarrow}|^2) K_1], \quad (6a)$$

$$\frac{dK_2}{d \ln \tau_c} = -2\tau_c^2 [(|t_{e\uparrow}|^2 - |t_{h\uparrow}|^2 - |t_{e\downarrow}|^2 + |t_{h\downarrow}|^2) + (|t_{e\uparrow}|^2 + |t_{h\uparrow}|^2 + |t_{e\downarrow}|^2 + |t_{h\downarrow}|^2) K_2], \quad (6b)$$

$$\frac{dt_\xi}{d \ln \tau_c} = \left[1 - \frac{(K_1 + \delta_{\xi,1})^2 + g(K_2 + \delta_{\xi,2})^2}{4g} \right] t_\xi, \quad (6c)$$

$$\frac{d\epsilon}{d \ln \tau_c} = \epsilon, \quad (6d)$$

where ξ -dependent charge pair $(\delta_{\xi,1}, \delta_{\xi,2})$ equals $(+1, +1)$, $(-1, -1)$, $(+1, -1)$, and $(-1, +1)$, respectively, when

$\xi = e \uparrow, h \uparrow, e \downarrow$, and $h \downarrow$. For simplicity, we begin with the fine-tuned situation where $\epsilon = 0$. Initially, $K_1 = K_2 = 0$, and all tunneling operators of Eq. (2) share the same scaling dimension [i.e., the factor after the minus sign of Eq. (6c)] $1/2 + r$. Following Eq. (6), the system flows to different fixed points depending on the symmetry among tunneling parameters t_ξ .

As the starting point, we look into the most generic situation and impose no requirement on tunneling parameters. Of this situation, absolute values of parameters K_1 and K_2 increase during the RG flow. Accompanying their enhancement, scaling dimension of the tunneling with the strongest amplitude begins to decrease, which in term induces an even stronger asymmetry or difference among tunnelings $\propto t_\xi$. To obtain a more intuitive understanding, we consider the fixed point where $t_{e\uparrow} \sim 1 \gg t_{e\downarrow}, t_{h\uparrow}, t_{h\downarrow}$, and $K_1 = K_2 = -1$. At this point, the leading process $\propto t_{e\uparrow}$ has a vanishing scaling dimension, and grows as if it was an energy cutoff. Consequently, at low enough temperatures, $t_{e\uparrow} \psi_\uparrow^\dagger a + \text{H.c.}$ becomes infinite, where ψ_\uparrow completely hybridizes the impurity ABS, and at meanwhile, suppresses the other communications between the ABS and the lead. A persistent lead-superconductor transport now has to rely on coherent Andreev tunneling $t_{e\uparrow} t_{h\downarrow} \psi_\uparrow^\dagger(0) \psi_\downarrow^\dagger(0) e^{-2i\varphi} a^\dagger a + \text{H.c.}$. As an Andreev tunneling consists of two coherent tunnelings [Fig. 2(b)], its low-energy feature is determined by the less relevant process $\propto t_{h\downarrow}$. Following Eq. (6), this process flows $dt_{h\downarrow}/d \ln \tau_c = -4rt_{h\downarrow}$ when $K_1 = K_2 = -1$, with the scaling dimension $1 + 4r$. This scaling dimension indicates that at low enough temperatures, the zero-bias conductance decreases following the temperature power law $G \propto T^{8r}$ and vanishes at zero temperature, different from the regular dissipation tunneling ($G \propto T^{2r}$) without superconductivity. As a reminder, the temperature power equals twice the difference between the scaling dimension and unity [70].

This $8r$ power law, however, requires perfect coherent Andreev reflections. In reality, the imperfection of the superconductor-proximitized nanowire induces possible transient states with the typical lifetime t_{imp} . Even when two subprocesses of an Andreev tunneling are coherent, the relaxation of two involved charges, during which dissipation is produced, might lose coherence in an imperfect nanowire [74]. Indeed, we consider the Andreev tunneling operator $\mathcal{O}_{\text{AR}} = \psi_\uparrow^\dagger a \exp(-i\varphi) \psi_\downarrow^\dagger a^\dagger \exp(-i\varphi) + \text{H.c.}$, whose correlation in time becomes

$$\langle \mathcal{O}_{\text{AR}}(t) \mathcal{O}_{\text{AR}}(0) \rangle = \langle H_{\text{T}}^0(t) H_{\text{T}}^0(0) \rangle \cdot \langle e^{-i\varphi(t+\delta t)} e^{-i\varphi(t+\delta t')} e^{i\varphi(\delta t)} e^{i\varphi(\delta t')} \rangle, \quad (7)$$

where $H_{\text{T}}^0 = \psi_\uparrow^\dagger a \psi_\downarrow^\dagger a^\dagger$ contains the lead operators, and $\delta t, \delta t' \sim t_{\text{imp}}$ refer to the incoherence-induced delay in time [72]. Their amplitudes determine the leading feature of the correlation Eq. (7). Indeed, when $t \gg t_{\text{imp}}$, the delay in time

becomes negligible, where the correlation of two dissipative phases $\propto t^{-8r}$. In contrast, the correlation changes to $\propto t^{-4r}$ for relatively shorter time $t \ll t_{\text{imp}}$. The correlation of phase is then determined by the cutoff in time, i.e., the inverse of the temperature $1/T$.

In the extreme case, when $t_{\text{imp}} \gg 1/T$, two phases become completely uncorrelated [72], thus reducing the suppression of conductance from dissipation by half [see Fig. 2(c)]. In this limit, Andreev reflection has the scaling dimension $1 + 2r$ instead, leading to the conductance power law $G \propto T^{4r}$. As a possible extension, the coherence-dependent conductance power law, which could potentially exist in other dissipative systems, provides us a possible tool in the detection of system coherence. In our system, incoherent power law might also occur in relatively high-temperature systems where the ABS has not been fully hybridized by the dominant lead operator. In this situation, an incoming electron might stay on the ABS for a long enough time during which the incoming electron and the reflected hole have become incoherent.

Conductance peaks.—Experimentally, two types of conductance peaks might be observed. First, and most interestingly, a Majorana resonance peak emerges when normal lead couples either to a topological MZM, or when the ABS consists of two spatially separated MZMs that decouple from each other (i.e., the quasi-MZM scenario predicted by, e.g., [77–81]) in case of a smooth lead-wire barrier [78]. Of both cases, the low-energy conductance can be obtained with the fact that they are self-dual systems [72]. More specifically, as the lead-Majorana coupling has the scaling dimension $r + 1/2$ initially, its dual operator at low temperatures has the scaling dimension $2/(1 + 2r)$, the inverse of the initial scaling. From that one arrives at the power law $2e^2/h - G \sim T^{(2-4r)/(1+2r)}$ that agrees with the result of Ref. [48], where tunneling to a real Majorana is considered.

Theoretically any dissipation is capable of killing generic (i.e., not fine-tuned) ABS peaks at low enough energies. However, in real experiments, ABS peaks might emerge when electron temperature is too high to witness the conductance suppression either from a weak dissipation or from a weak asymmetry among tunneling parameters. Nevertheless, we expect the absence of universal scaling behaviors near these ABS peaks, as they do not correspond to fixed points of RG equations [Eq. (6)]. We emphasize that the missing of universality near the ABS peak does not contradict the materials of Table I, where scaling behaviors are only predicted near the zero-conductance fixed point, at low enough temperatures. For instance, we study the case where $t_{e\uparrow} = 0.25$ is slightly larger than $t_{h\downarrow}$ and much larger than the other two parameters. In this situation the system conductance and its dependence on temperature are mostly determined by $t_{h\downarrow}$. In Fig. 3, we thus plot $t_{h\downarrow}$ and its scaling dimension $D(t_{h\downarrow})$ [i.e., $(K_1 - 1)^2/4g + (K_2 + 1)^2/4$ of Eq. (6c)] to indirectly investigate the conductance features.

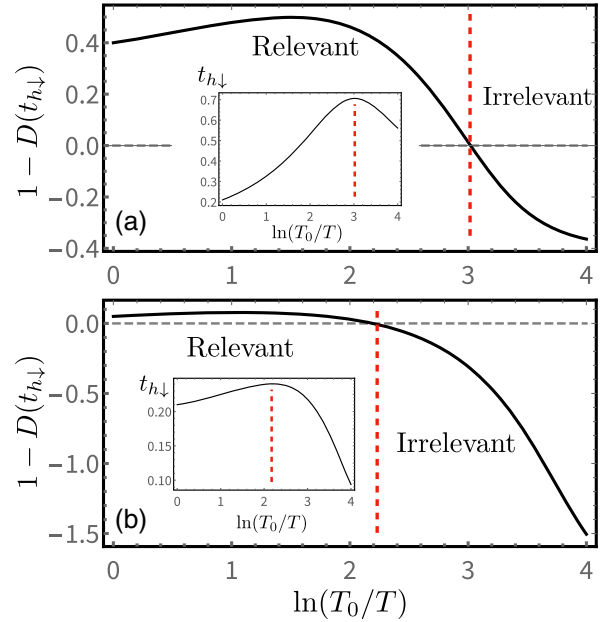


FIG. 3. Scaling dimension and amplitude (inset) of the operator $\propto t_{h\downarrow}$, when $t_{e\uparrow}$ is dominating. Temperature decreases when value of x axis increases. (a) When $r = 0.1$, $t_{h\downarrow}$ becomes RG irrelevant when $T \approx 0.05T_0$, with the peak height ≈ 0.7 . (b) When $r = 0.45$, the ABS conductance arrives at its peak position much faster $T \approx 0.11T_0$, with a much smaller peak height ≈ 0.24 . Other parameters in (a) and (b) are the same.

In our example, $D(t_{h\downarrow})$ strongly determines how the system conductance changes as a function of the energy, i.e., the larger one of temperature and bias. Pedagogically, when $D(t_{h\downarrow}) > 1$ [$D(t_{h\downarrow}) < 1$], the tunneling operator is irrelevant (relevant) and conductance increases (decreases) when energy increases. Conductance peak or dip then appears when $D(t_{h\downarrow}) = 1$. In Fig. 3(a), for a weak dissipation $r = 0.1$, the conductance arrives at its peak value [where $D(t_{h\downarrow}) = 1$] when $T \approx 0.05T_0$, where T_0 refers to temperature at which RG starts. However, near this peak position, $D(t_{h\downarrow})$ keeps changing with temperature, indicating the absence of universality, i.e., persuasive temperature power laws of conductance under low enough energies. For a stronger dissipation $r = 0.45$ (while fixing other parameters) shown in Fig. 3(b), the tunneling $\propto t_{h\downarrow}$ becomes irrelevant in a larger regime ($T < 0.11T_0$), indicating a more strongly suppressed ABS tunneling.

Briefly, in contrast to a Majorana zero-bias peak, ABS zero-bias peaks do not have a universal height, and in most cases do not necessarily display universality in higher temperature [72]. Indeed, following Table I, generic ABS conductance curves display universality only when the system flows close enough to the low temperature fixed point. While our results suggest that a stronger dissipation (larger r but smaller than 0.5) can more easily suppress the ABS peak and provide a sharp difference compared with Majorana peak.

Detuned ABS and multiple-ABS scenarios.—In real experiment, scaling dimensions listed in Table I, which are among our central conclusions, should be checked carefully, as (i) the ABS energy might be finite; (ii) multiple on-resonance ABSs might talk to the lead simultaneously, and (iii) a Majorana might become surrounded by multiple ABSs [58].

As the response to the concern (i), we notice that the ABS detuning Hamiltonian $H_{\text{ABS}} = \epsilon a^\dagger a$ is highly RG relevant from Eq. (6d). The detuning energy should thus be considered as another possible low-energy cutoff, in addition to temperature T for the zero-bias situation. Consequently, if $T \gg \epsilon$, RG flow does not see the coupling ϵ , and the conductance behavior then coincides with that when $\epsilon = 0$. In the opposite limit $T \ll \epsilon$ the single-electron tunneling (e.g., $\psi_\uparrow^\dagger a$) requires an extra energy, and is thus suppressed. In both limits, Andreev tunneling dominates at low temperatures, leading to the same temperature dependence as shown in Table I. Finally, the crossover $T \sim \epsilon$ is not within the universality class, and conductance should not follow any temperature power law. The concern (ii), i.e., the multi-ABS scenario, can be visited following the statement that the system prefers ground state with lower degeneracy [82]. Then, only a single ABS will dominate the Andreev reflection. The result is once again the same as in Table I.

The situation becomes most interesting if the superconductor hosts a single MZM (either topological or quasi) and one or multiple generic ABSs. At lowest energies, the system behavior can be obtained from our analysis above on the multi-ABS scenario: all ABSs become decoupled or hybridized, and lead-wire charge transport relies on tunneling into the MZM. Consequently, for generic cases, we expect the same low-temperature behavior as the MZM situation of Table I, given low enough temperatures. However, how the system arrives at this fixed point might depend on, e.g., the relative amplitudes of the lead-ABS and the lead-MZM couplings. Indeed, when lead-ABS coupling is stronger at high temperatures, one might expect the nontrivial transition from ABS-like (conductance-suppression) to MZM-like (conductance-enhancement) scaling behaviors when the temperature decreases.

Finally, we emphasize that our theory is experimentally applicable to the hybrid nanowire (i.e., Fig. 1) and potentially to other ABS and/or MZM platforms using scanning tunneling microscope detection [63]. To date, our predictions on major features (conductance power laws in Table I) of dissipative tunneling into ABSs of a hybrid nanowire have been experimentally demonstrated by a jointly submitted work, Ref. [83], for a sample with $r \approx 0.22$. Following this Letter, ABS-induced zero-bias conductance peaks in dissipation-free systems are suppressed (by dissipation) into valleys with typical conductance values beneath $0.1 \times 2e^2/h$ for temperatures below 100 mK. It is thus reasonable to seek for MZM signatures

in samples with r around 0.22, and temperatures between 10 and 100 mK.

We thank Xin Liu, Fuchun Zhang, Harold Baranger and Gleb Finkelstein for helpful discussions. The work is supported by Natural Science Foundation of China (Grants No. 11974198 and 12004040) and Tsinghua University Initiative Scientific Research Program.

D. L and G. Z. contributed equally to this work.

*Corresponding author.

dongeliu@mail.tsinghua.edu.cn

- [1] E. L. Wolf, *Principles of Electron Tunneling Spectroscopy* (Oxford University Press, New York, 2012), Vol. 152.
- [2] N. Read and D. Green, *Phys. Rev. B* **61**, 10267 (2000).
- [3] A. Y. Kitaev, *Phys. Usp.* **44**, 131 (2001).
- [4] R. M. Lutchyn, J. D. Sau, and S. Das Sarma, *Phys. Rev. Lett.* **105**, 077001 (2010).
- [5] Y. Oreg, G. Refael, and F. Von Oppen, *Phys. Rev. Lett.* **105**, 177002 (2010).
- [6] R. M. Lutchyn, E. P. Bakkers, L. P. Kouwenhoven, P. Krogstrup, C. M. Marcus, and Y. Oreg, *Nat. Rev. Mater.* **3**, 52 (2018).
- [7] K. Sengupta, I. Žutić, H.-J. Kwon, V. M. Yakovenko, and S. Das Sarma, *Phys. Rev. B* **63**, 144531 (2001).
- [8] K. T. Law, P. A. Lee, and T. K. Ng, *Phys. Rev. Lett.* **103**, 237001 (2009).
- [9] K. Flensberg, *Phys. Rev. B* **82**, 180516(R) (2010).
- [10] M. Wimmer, A. Akhmerov, J. Dahlhaus, and C. Beenakker, *New J. Phys.* **13**, 053016 (2011).
- [11] V. Mourik, K. Zuo, S. M. Frolov, S. R. Plissard, E. P. A. M. Bakkers, and L. P. Kouwenhoven, *Science* **336**, 1003 (2012).
- [12] M. T. Deng, C. Yu, G. Huang, M. Larsson, P. Caroff, and H. Xu, *Nano Lett.* **12**, 6414 (2012).
- [13] A. Das, Y. Ronen, Y. Most, Y. Oreg, M. Heiblum, and H. Shtrikman, *Nat. Phys.* **8**, 887 (2012).
- [14] A. D. K. Finck, D. J. Van Harlingen, P. K. Mohseni, K. Jung, and X. Li, *Phys. Rev. Lett.* **110**, 126406 (2013).
- [15] H. O. H. Churchill, V. Fatemi, K. Grove-Rasmussen, M. T. Deng, P. Caroff, H. Q. Xu, and C. M. Marcus, *Phys. Rev. B* **87**, 241401(R) (2013).
- [16] M. Deng, S. Vaitiekėnas, E. B. Hansen, J. Danon, M. Leijnse, K. Flensberg, J. Nygård, P. Krogstrup, and C. M. Marcus, *Science* **354**, 1557 (2016).
- [17] H. Zhang *et al.*, *Nat. Commun.* **8**, 16025 (2017).
- [18] J. Chen, P. Yu, J. Stenger, M. Hocevar, D. Car, S. R. Plissard, E. P. Bakkers, T. D. Stanescu, and S. M. Frolov, *Sci. Adv.* **3**, e1701476 (2017).
- [19] H. J. Suominen, M. Kjaergaard, A. R. Hamilton, J. Shabani, C. J. Palmstrøm, C. M. Marcus, and F. Nichele, *Phys. Rev. Lett.* **119**, 176805 (2017).
- [20] F. Nichele, A. C. C. Drachmann, A. M. Whiticar, E. C. T. O'Farrell, H. J. Suominen, A. Fornieri, T. Wang, G. C. Gardner, C. Thomas, A. T. Hatke, P. Krogstrup, M. J. Manfra, K. Flensberg, and C. M. Marcus, *Phys. Rev. Lett.* **119**, 136803 (2017).

- [21] Ö. Gül, H. Zhang, J. D. S. Bommer, M. W. A. de Moor, D. Car, S. R. Plissard, E. P. A. M. Bakkers, A. Geresdi, K. Watanabe, T. Taniguchi, and L. P. Kouwenhoven, *Nat. Nanotechnol.* **13**, 192 (2018).
- [22] S. Vaitiekėnas, M.-T. Deng, J. Nygård, P. Krogstrup, and C. M. Marcus, *Phys. Rev. Lett.* **121**, 037703 (2018).
- [23] M. W. de Moor, J. D. Bommer, D. Xu, G. W. Winkler, A. E. Antipov, A. Bargerbos, G. Wang, N. van Loo, R. L. Veld, S. Gazibegovic *et al.*, *New J. Phys.* **20**, 103049 (2018).
- [24] J. D. S. Bommer, H. Zhang, O. Gül, B. Nijholt, M. Wimmer, F. N. Rybakov, J. Garaud, D. Rodic, E. Babaev, M. Troyer, D. Car, S. R. Plissard, E. P. A. M. Bakkers, K. Watanabe, T. Taniguchi, and L. P. Kouwenhoven, *Phys. Rev. Lett.* **122**, 187702 (2019).
- [25] A. Grivnin, E. Bor, M. Heiblum, Y. Oreg, and H. Shtrikman, *Nat. Commun.* **10**, 1940 (2019).
- [26] D. Pan, H. Song, S. Zhang, L. Liu, L. Wen, D. Liao, R. Zhuo, Z. Wang, Z. Zhang, S. Yang, J. Ying, W. Miao, Y. Li, R. Shang, H. Zhang, and J. Zhao, [arXiv:2011.13620](https://arxiv.org/abs/2011.13620).
- [27] H. Zhang, M. W. de Moor, J. D. Bommer, D. Xu, G. Wang, N. van Loo, C.-X. Liu, S. Gazibegovic, J. A. Logan, D. Car *et al.*, [arXiv:2101.11456](https://arxiv.org/abs/2101.11456).
- [28] H. Song, Z. Zhang, D. Pan, D. Liu, Z. Wang, Z. Cao, L. Liu, L. Wen, D. Liao, R. Zhuo *et al.*, [arXiv:2107.08282](https://arxiv.org/abs/2107.08282).
- [29] F. Pientka, G. Kells, A. Romito, P. W. Brouwer, and F. von Oppen, *Phys. Rev. Lett.* **109**, 227006 (2012).
- [30] J. Liu, A. C. Potter, K. T. Law, and P. A. Lee, *Phys. Rev. Lett.* **109**, 267002 (2012).
- [31] W. S. Cole, J. D. Sau, and S. Das Sarma, *Phys. Rev. B* **94**, 140505(R) (2016).
- [32] C.-X. Liu, J. D. Sau, T. D. Stanescu, and S. Das Sarma, *Phys. Rev. B* **96**, 075161 (2017).
- [33] D. E. Liu, E. Rossi, and R. M. Lutchyn, *Phys. Rev. B* **97**, 161408(R) (2018).
- [34] Z. Cao, H. Zhang, H.-F. Lü, W.-X. He, H.-Z. Lu, and X. C. Xie, *Phys. Rev. Lett.* **122**, 147701 (2019).
- [35] H. Pan and S. Das Sarma, *Phys. Rev. Research* **2**, 013377 (2020).
- [36] S. Das Sarma and H. Pan, *Phys. Rev. B* **103**, 195158 (2021).
- [37] H. Pan, C.-X. Liu, M. Wimmer, and S. Das Sarma, *Phys. Rev. B* **103**, 214502 (2021).
- [38] J. Cardy, *Scaling and Renormalization in Statistical Physics* (Cambridge University Press, Cambridge, England, 1996), Vol. 5.
- [39] G.-L. Ingold and Y. V. Nazarov, in *Single Charge Tunneling* (Springer, New York, 1992), pp. 21–107.
- [40] H. T. Mebrahtu, I. V. Borzenets, D. E. Liu, H. Zheng, Y. V. Bomze, A. I. Smirnov, H. U. Baranger, and G. Finkelstein, *Nature (London)* **488**, 61 (2012).
- [41] H. T. Mebrahtu, I. V. Borzenets, H. Zheng, Y. V. Bomze, A. I. Smirnov, S. Florens, H. U. Baranger, and G. Finkelstein, *Nat. Phys.* **9**, 732 (2013).
- [42] S. Jezouin, M. Albert, F. D. Parmentier, A. Anthore, U. Gennser, A. Cavanna, I. Safi, and F. Pierre, *Nat. Commun.* **4**, 1802 (2013).
- [43] A. Anthore, Z. Iftikhar, E. Boulat, F. D. Parmentier, A. Cavanna, A. Ouerghi, U. Gennser, and F. Pierre, *Phys. Rev. X* **8**, 031075 (2018).
- [44] K. A. Matveev and L. I. Glazman, *Phys. Rev. Lett.* **70**, 990 (1993).
- [45] I. Safi and H. Saleur, *Phys. Rev. Lett.* **93**, 126602 (2004).
- [46] K. Le Hur and M.-R. Li, *Phys. Rev. B* **72**, 073305 (2005).
- [47] S. Florens, P. Simon, S. Andergassen, and D. Feinberg, *Phys. Rev. B* **75**, 155321 (2007).
- [48] D. E. Liu, *Phys. Rev. Lett.* **111**, 207003 (2013).
- [49] D. E. Liu, H. Zheng, G. Finkelstein, and H. U. Baranger, *Phys. Rev. B* **89**, 085116 (2014).
- [50] H. Zheng, S. Florens, and H. U. Baranger, *Phys. Rev. B* **89**, 235135 (2014).
- [51] K. Wölms and K. Flensberg, *Phys. Rev. B* **92**, 165428 (2015).
- [52] G. Zhang, E. Novais, and H. U. Baranger, *Phys. Rev. Lett.* **118**, 050402 (2017).
- [53] K. Le Hur, L. Henriot, L. Herviou, K. Plekhanov, A. Petrescu, T. Goren, M. Schiro, C. Mora, and P. P. Orth, *C. R. Phys.* **19**, 451 (2018).
- [54] D. Liu, Z. Cao, H. Zhang, and D. E. Liu, *Phys. Rev. B* **101**, 081406(R) (2020).
- [55] G. Zhang and C. Spånslätt, *Phys. Rev. B* **102**, 045111 (2020).
- [56] G. Zhang, E. Novais, and H. U. Baranger, *Phys. Rev. B* **104**, 165423 (2021).
- [57] C. Zeng, G. Sharma, S. Tewari, and T. Stanescu, [arXiv:2105.06469](https://arxiv.org/abs/2105.06469).
- [58] H.-H. Sun, K.-W. Zhang, L.-H. Hu, C. Li, G.-Y. Wang, H.-Y. Ma, Z.-A. Xu, C.-L. Gao, D.-D. Guan, Y.-Y. Li, C. Liu, D. Qian, Y. Zhou, L. Fu, S.-C. Li, F.-C. Zhang, and J.-F. Jia, *Phys. Rev. Lett.* **116**, 257003 (2016).
- [59] D. Wang, L. Kong, P. Fan, H. Chen, S. Zhu, W. Liu, L. Cao, Y. Sun, S. Du, J. Schneeloch, R. Zhong, G. Gu, L. Fu, H. Ding, and H.-J. Gao, *Science* **362**, 333 (2018).
- [60] Q. Liu, C. Chen, T. Zhang, R. Peng, Y.-J. Yan, Chen-Hao-Ping Wen, X. Lou, Y.-L. Huang, J.-P. Tian, X.-L. Dong, G.-W. Wang, W.-C. Bao, Q.-H. Wang, Z.-P. Yin, Z.-X. Zhao, and D.-L. Feng, *Phys. Rev. X* **8**, 041056 (2018).
- [61] L. Kong, S. Zhu, M. Papaj, H. Chen, L. Cao, H. Isobe, Y. Xing, W. Liu, D. Wang, P. Fan, Y. Sun, S. Du, J. Schneeloch, R. Zhong, G. Gu, L. Fu, H.-J. Gao, and H. Ding, *Nat. Phys.* **15**, 1181 (2019).
- [62] T. Machida, Y. Sun, S. Pyon, S. Takeda, Y. Kohsaka, T. Hanaguri, T. Sasagawa, and T. Tamegai, *Nat. Mater.* **18**, 811 (2019).
- [63] C. Brun, K. H. Müller, I.-Po. Hong, F. Patthey, C. Flindt, and W.-D. Schneider, *Phys. Rev. Lett.* **108**, 126802 (2012).
- [64] A. J. Leggett, S. Chakravarty, A. T. Dorsey, M. P. Fisher, A. Garg, and W. Zwerger, *Rev. Mod. Phys.* **59**, 1 (1987).
- [65] A. O. Caldeira and A. J. Leggett, *Phys. Rev. Lett.* **46**, 211 (1981).
- [66] Y. Tanaka and S. Kashiwaya, *Phys. Rev. B* **70**, 012507 (2004).
- [67] T. Giamarchi, *Quantum Physics in One Dimension* (Oxford University Press, New York, 2003).
- [68] P. W. Anderson, G. Yuval, and D. Hamann, *Phys. Rev. B* **1**, 4464 (1970).
- [69] C. L. Kane and M. P. A. Fisher, *Phys. Rev. B* **46**, 7268 (1992).

- [70] C. L. Kane and M. P. A. Fisher, *Phys. Rev. B* **46**, 15233 (1992).
- [71] A. Furusaki and N. Nagaosa, *Phys. Rev. B* **47**, 3827 (1993).
- [72] See Supplemental Material at <http://link.aps.org/supplemental/10.1103/PhysRevLett.128.076802> for details of the derivation.
- [73] U. Weiss, *Quantum Dissipative Systems*, 4th ed. (World Scientific, Singapore, 2012).
- [74] Here, we do not break the coherence of two subprocesses of a single Andreev tunneling. This is similar to the incoherence Andreev reflection in nonequilibrium setups [75,76], where decoherence only emerges between different Andreev reflection processes.
- [75] E. V. Bezuglyi, E. N. Bratus', V. S. Shumeiko, and G. Wendin, *Phys. Rev. Lett.* **83**, 2050 (1999).
- [76] S. Duhot, F. Lefloch, and M. Houzet, *Phys. Rev. Lett.* **102**, 086804 (2009).
- [77] E. Prada, P. San-Jose, and R. Aguado, *Phys. Rev. B* **86**, 180503(R) (2012).
- [78] G. Kells, D. Meidan, and P. W. Brouwer, *Phys. Rev. B* **86**, 100503(R) (2012).
- [79] C. Moore, T. D. Stanescu, and S. Tewari, *Phys. Rev. B* **97**, 165302 (2018).
- [80] C. Moore, C. Zeng, T. D. Stanescu, and S. Tewari, *Phys. Rev. B* **98**, 155314 (2018).
- [81] A. Vuik, B. Nijholt, A. R. Akhmerov, and M. Wimmer, *SciPost Phys* **7**, 061 (2019).
- [82] I. Affleck and A. W. W. Ludwig, *Phys. Rev. Lett.* **67**, 161 (1991).
- [83] S. Zhang, Z. Wang, D. Pan, H. Li, S. Lu, Z. Li, G. Zhang, D. Liu, Z. Cao, L. Liu, L. Wen, D. Liao, R. Zhuo, R. Shang, D. E. Liu, J. Zhao, and H. Zhang, following Letter, *Phys. Rev. Lett.* **128**, 076803 (2022).